



# A new temperature stable microwave dielectric with low-firing temperature in $\text{Bi}_2\text{MoO}_6\text{-TiO}_2$ system

Li-Xia Pang<sup>a,\*</sup>, Hong Wang<sup>a,\*</sup>, Di Zhou<sup>a</sup>, Xi Yao<sup>a</sup>

<sup>a</sup> Electronic Materials Research Laboratory, Key Laboratory of the Ministry of Education, Xi'an Jiaotong University, Xi'an 710049, China

## ARTICLE INFO

### Article history:

Received 5 November 2009  
Received in revised form  
19 December 2009  
Accepted 26 December 2009  
Available online 4 January 2010

### Keywords:

Microwave dielectric  
LTCC  
 $\text{xBi}_2\text{MoO}_6\text{-(1-x)TiO}_2$

## ABSTRACT

A new temperature stable microwave dielectric with low-firing temperature in  $\text{xBi}_2\text{MoO}_6\text{-(1-x)TiO}_2$  system was prepared by conventional solid state reaction method. The crystalline phases, sintering behavior, microwave dielectric properties of  $\text{xBi}_2\text{MoO}_6\text{-(1-x)TiO}_2$  ceramics were studied. All the  $\text{xBi}_2\text{MoO}_6\text{-(1-x)TiO}_2$  ceramics could be well sintered at 850 °C for 3 h. X-ray diffraction analysis showed that tetragonal rutile phase and monoclinic  $\text{Bi}_2\text{MoO}_6$  phase coexisted in the ceramic. The permittivity  $\epsilon_r$  changed from 77.5 to 33.5 and the temperature coefficient of resonant frequency  $\tau_f$  value shifted from +348.1 to -37.8 ppm/°C as the  $x$  value increased from 0.06 to 0.65. The temperature stable microwave dielectric ceramic was obtained when  $x=0.57$  in the  $\text{xBi}_2\text{MoO}_6\text{-(1-x)TiO}_2$  system, and it showed excellent dielectric properties of  $\epsilon_r=36.7$ ,  $Qf=16,800$  GHz and  $\tau_f=0$  ppm/°C.

Crown Copyright © 2010 Published by Elsevier B.V. All rights reserved.

## 1. Introduction

With the rapid development of mobile communication and satellite communication, microwave electronic devices are required to be developed and fabricated for miniaturization and integration. The low temperature co-fired ceramic technology (LTCC) becomes an important fabricating technology that can integrate the passive components within a monolithic bulk module with IC chips mounted on its surface. As microwave dielectric, high quality factor ( $Qf$ ), near zero temperature coefficient of resonant frequency ( $\tau_f$ ), and low-firing temperature (<961 °C, the melting temperature of Ag electrode) are essential for practical application. In addition, high relative permittivity ( $\epsilon_r > 20$ ) is preferred for miniaturization [1–3]. Up to now, large numbers of materials have been developed with excellent microwave dielectric properties, while most of them possess high sintering temperatures ( $\geq 1000$  °C). Recently, a number of material researchers have focused their research on lowering the sintering temperatures of microwave dielectric ceramics to meet the LTCC requirements. Three approaches are usually used to develop low-firing microwave dielectric ceramics: (a) addition of oxides or glass with low melting temperature [4–11], such as  $\text{V}_2\text{O}_5$ , CuO, LiF,

and  $\text{B}_2\text{O}_3$ ; (b) utilization of ultra-fine particles for raw materials [12,13]; (c) development of novel glass-free low-firing dielectric ceramics, including  $\text{Bi}_2\text{O}_3\text{-TeO}_2$ ,  $\text{TiO}_2\text{-TeO}_2$ ,  $\text{CaO-TeO}_2$ ,  $\text{BaO-TeO}_2$ ,  $\text{ZnO-TeO}_2$  binary systems,  $\text{BaO-TiO}_2\text{-TeO}_2$  ternary system, and  $\text{Bi}_2\text{W}_2\text{O}_9$  systems [14–21]. Our recent research [22] showed that  $\text{Bi}_2\text{O}_3\text{-MoO}_3$  binary system is a new ultra-low-firing microwave dielectric material.  $\text{Bi}_2\text{Mo}_3\text{O}_{12}$ ,  $\text{Bi}_2\text{Mo}_2\text{O}_9$ , and  $\text{Bi}_2\text{MoO}_6$  are the single phases in the  $\text{Bi}_2\text{O}_3\text{-MoO}_3$  system and all of them show excellent microwave dielectric properties. Rutile  $\text{TiO}_2$  is a good high  $K$  (permittivity) microwave dielectric with dielectric constant (105), high quality factor (9200 at 5 GHz), and large positive  $\tau_f$  value (+465 ppm/°C) [23]. In this work, rutile  $\text{TiO}_2$  was chosen to compensate [20,21,24,25] the negative  $\tau_f$  value of  $\text{Bi}_2\text{MoO}_6$  which possess high permittivity (31), high  $Qf$  value (16,700 GHz), and negative  $\tau_f$  value (-114 ppm/°C) [22]. The compounds  $\text{xBi}_2\text{MoO}_6\text{-(1-x)TiO}_2$  ( $x=0.06, 0.125, 0.21, 0.33, 0.50, 0.57, 0.65$ ) were prepared by conventional solid state reaction method. The chemical compatibility, sintering behavior, and microwave dielectric properties were studied.

## 2. Experimental

Proportionate amounts of reagent-grade starting materials of  $\text{Bi}_2\text{O}_3$  (>99%, Shu-Du Powders Co. Ltd., Chengdu, China),  $\text{MoO}_3$  (>99%, Fuchen Chemical Reagents, Tianjin, China) and rutile  $\text{TiO}_2$  (>99%, Linghua Co. Ltd., Zhaoqing, China) were prepared by mixed-oxide method according to the stoichiometrics  $\text{xBi}_2\text{MoO}_6\text{-(1-x)TiO}_2$  ( $x=0.06, 0.125, 0.21, 0.33, 0.50, 0.57, 0.65$ ). The final powders were calcined at a temperature between 700 and 800 °C for 5 h and the cylinder specimens (10 mm in diameter and 5 mm in height) were sintered in air at temperatures between 800 and 900 °C for 3 h.

\* Corresponding authors at: Electronic Materials Research Laboratory, Key Laboratory of the Ministry of Education, Xi'an Jiaotong University, Xi'an 710049, China. Tel.: +86 2982668679; fax: +86 2982668794.

E-mail addresses: [plx1982@gmail.com](mailto:plx1982@gmail.com) (L.-X. Pang), [hwang@mail.xjtu.edu.cn](mailto:hwang@mail.xjtu.edu.cn) (H. Wang).

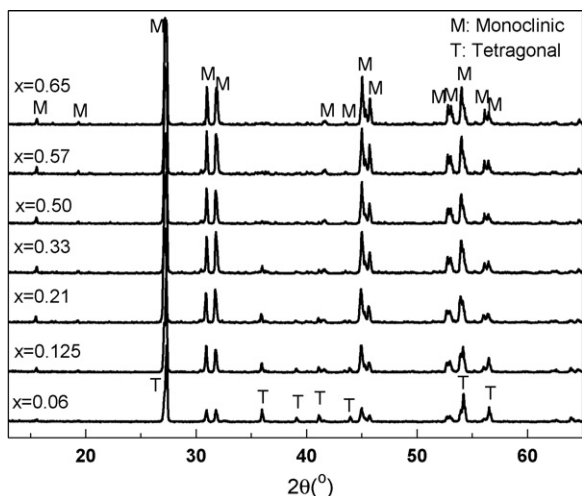


**Fig. 1.** X-ray diffraction patterns of  $x\text{Bi}_2\text{MoO}_6-(1-x)\text{TiO}_2$  compounds sintered at  $850^\circ\text{C}$  for 3 h. (T: Tetragonal rutile phase; O: Monoclinic  $\text{Bi}_2\text{MoO}_6$  phase).

The crystalline phases were investigated using X-ray diffraction (XRD) with Cu  $K\alpha$  radiation (Rigaku D/MAX-2400 X-ray diffractometry, Tokyo, Japan). The microstructures were observed on the fracture surfaces with scanning electron microscopy (SEM) (JSM-6460, JEOL, Tokyo, Japan) coupled with energy-dispersive X-ray spectroscopy (EDS). The apparent densities were measured by Archimedes' method. The dielectric properties were measured at microwave frequency by the  $\text{TE}_{018}$  shielded cavity method with a network analyzer (8720ES, Agilent, Palo Alto, CA) and a temperature chamber (Delta 9023, Delta Design, Poway, CA). The  $\tau_f$  value was calculated by the following formula:

$$\tau_f = \frac{f_{85} - f_{25}}{f_{25}(85 - 25)} 10^6 \text{ (ppm/}^\circ\text{C)} \quad (1)$$

where  $f_{85}$  and  $f_{25}$  were the  $\text{TE}_{018}$  resonant frequencies at 85 and  $25^\circ\text{C}$ , respectively.

### 3. Results and discussion

The X-ray diffraction patterns of  $x\text{Bi}_2\text{MoO}_6-(1-x)\text{TiO}_2$  compounds sintered at  $850^\circ\text{C}$  are shown in Fig. 1. Diffraction peaks of both tetragonal rutile phase and monoclinic  $\text{Bi}_2\text{MoO}_6$  phase present in the  $x\text{Bi}_2\text{MoO}_6-(1-x)\text{TiO}_2$  specimens, which means that the  $\text{Bi}_2\text{MoO}_6$  phase could coexist with rutile  $\text{TiO}_2$  phase. With the content of  $\text{Bi}_2\text{MoO}_6$  increasing in the compound, the intensities of the diffraction peaks of  $\text{Bi}_2\text{MoO}_6$  phase increased greatly. When  $x$  value increased to 0.5, the diffraction peaks of rutile  $\text{TiO}_2$  phase could barely be detected because of the low volume fraction of  $\text{TiO}_2$  phase.

To investigate the microstructures of the sintered  $x\text{Bi}_2\text{MoO}_6-(1-x)\text{TiO}_2$  ceramics and to obtain the volume fractions of the  $\text{Bi}_2\text{MoO}_6$  phase in the compounds, the backscattered electron images of the fractured surfaces of  $x\text{Bi}_2\text{MoO}_6-(1-x)\text{TiO}_2$  ceramics are shown in Fig. 2. There were two kinds of grains in

the ceramic matrixes, the dark ones with smaller grain size and the light ones with bigger grain size. EDS patterns in Fig. 2(h) showed that the dark grains were Ti-rich and in the light grains the amount of Bi was nearly two times of Mo. Associating with the XRD analysis in Fig. 1, it can be concluded that the dark and the light grains were the tetragonal rutile and the monoclinic  $\text{Bi}_2\text{MoO}_6$  grains, respectively. Because of the great difference in the sintering temperature between pure rutile  $\text{TiO}_2$  ceramic [23] and  $\text{Bi}_2\text{MoO}_6$  ceramic [22], the rutile grains were smaller and with regular shape, and the  $\text{Bi}_2\text{MoO}_6$  grains were bigger and showed irregular shape. The amount of  $\text{Bi}_2\text{MoO}_6$  phase increased greatly as the  $x$  value increased from 0.06 to 0.500. The volume fractions of  $\text{Bi}_2\text{MoO}_6$  phase in the ceramic matrixes were obtained from the backscattered electron images in Fig. 2. The measured and the theoretical volume fractions of  $\text{Bi}_2\text{MoO}_6$  phase are shown in Fig. 3. It shows that the measured volume fractions of  $\text{Bi}_2\text{MoO}_6$  phase were a little higher than the theoretical values when the content of  $\text{Bi}_2\text{MoO}_6$  was as high as  $x=0.21$  in the compounds. Combining with the EDS analysis in Fig. 2(h), it is concluded that the Ti element infiltrated slightly into the  $\text{Bi}_2\text{MoO}_6$  grains and a solid solution with  $\text{Bi}_2\text{MoO}_6$  phase formed in the compound.

Fig. 4 presents the bulk densities, theoretical densities and relative densities of the  $x\text{Bi}_2\text{MoO}_6-(1-x)\text{TiO}_2$  composite ceramics sintered at  $850^\circ\text{C}$  for 3 h. The relative densities of all the specimens were above 95%, suggesting that dense ceramics were obtained after sintering at  $850^\circ\text{C}$ .

Table 1 shows the theoretical and the measured microwave dielectric properties of the  $x\text{Bi}_2\text{MoO}_6-(1-x)\text{TiO}_2$  composite ceramics. The theoretical permittivity ( $\epsilon_r$ ) of the composite ceramic was obtained from the well-known Lichtenecker empirical logarithmic rule [26],

$$\lg \epsilon = y_1 \lg \epsilon_1 + y_2 \lg \epsilon_2 \quad (2)$$

where  $y_1$  and  $y_2$  are the volume fractions;  $\epsilon_1$  and  $\epsilon_2$  are the permittivities of the  $\text{Bi}_2\text{MoO}_6$  ceramic and the rutile  $\text{TiO}_2$  ceramic respectively. It is seen from Table 1 that the measured permittivity of the  $x\text{Bi}_2\text{MoO}_6-(1-x)\text{TiO}_2$  composite ceramic agreed well with the theoretical value. It decreased linearly from 77.5 to 35.5 as the  $x$  value increased from 0.06 to 0.65. The Qf values of the  $x\text{Bi}_2\text{MoO}_6-(1-x)\text{TiO}_2$  compounds were in the range between 14,500 and 16,800 GHz. As well known, microwave dielectric loss includes two parts: intrinsic loss and extrinsic loss. Intrinsic losses were caused by absorptions of phonon oscillation and extrinsic losses were caused by lattice defects (impurity, cavity, substitution, grain boundaries, size and shapes of grains, second phase, pores, etc.) [27,28]. In the  $x\text{Bi}_2\text{MoO}_6-(1-x)\text{TiO}_2$  composite ceramics, the influence from the intrinsic factors might be shielded by the extrinsic ones. As a result it shows no direct relation between the Qf value and the composition.

**Table 1**  
Microwave dielectric properties of  $x\text{Bi}_2\text{MoO}_6-(1-x)\text{TiO}_2$  composite ceramics.

| Compounds    | $\epsilon_r$ (theo.) | $\epsilon_r$ (meas.) | Qf (GHz)         | $\tau_f$ (theo.) (ppm/ $^\circ\text{C}$ ) | $\tau_f$ (meas.) (ppm/ $^\circ\text{C}$ ) |
|--------------|----------------------|----------------------|------------------|---|---|
| $x=0.0$ [20] |                      | 105                  | 46,000           | –   | +465                                      |
| $x=0.06$     | 81.8                 | $78 \pm 1.0$         | $15,000 \pm 500$ | +347.5                                    | $+348.1 \pm 7.0$                          |
| $x=0.125$    | 65.6                 | $65.0 \pm 0.7$       | $16,818 \pm 100$ | +243.9                                    | $+314.5 \pm 6.0$                          |
| $x=0.21$     | 53.9                 | $54.5 \pm 0.5$       | $16,350 \pm 100$ | +151.7                                    | $+207.3 \pm 4.5$                          |
| $x=0.33$     | 45.2                 | $46.2 \pm 0.6$       | $14,500 \pm 300$ | +69.2                                     | $+87.8 \pm 3.0$                           |
| $x=0.50$     | 38.6                 | $38.5 \pm 0.9$       | $15,020 \pm 100$ | –5.1                                      | $+47.5 \pm 2.5$                           |
| $x=0.57$     | 36.7                 | $36.7 \pm 0.9$       | $16,800 \pm 200$ | –28.3                                     | $–0.0 \pm 1.0$                            |
| $x=0.65$     | 35.0                 | $35.5 \pm 0.5$       | $15,034 \pm 300$ | –50.7                                     | $–37.8 \pm 1.5$                           |
| $x=1.0$ [19] |                      | 31                   | 1,6700           | –   | –114                                      |

$\epsilon_r$  (theo.): theoretical permittivity;  $\epsilon_r$  (meas.): measured permittivity.

$\tau_f$  (theo.): theoretical  $\tau_f$  value;  $\tau_f$  (meas.): measured  $\tau_f$  value.

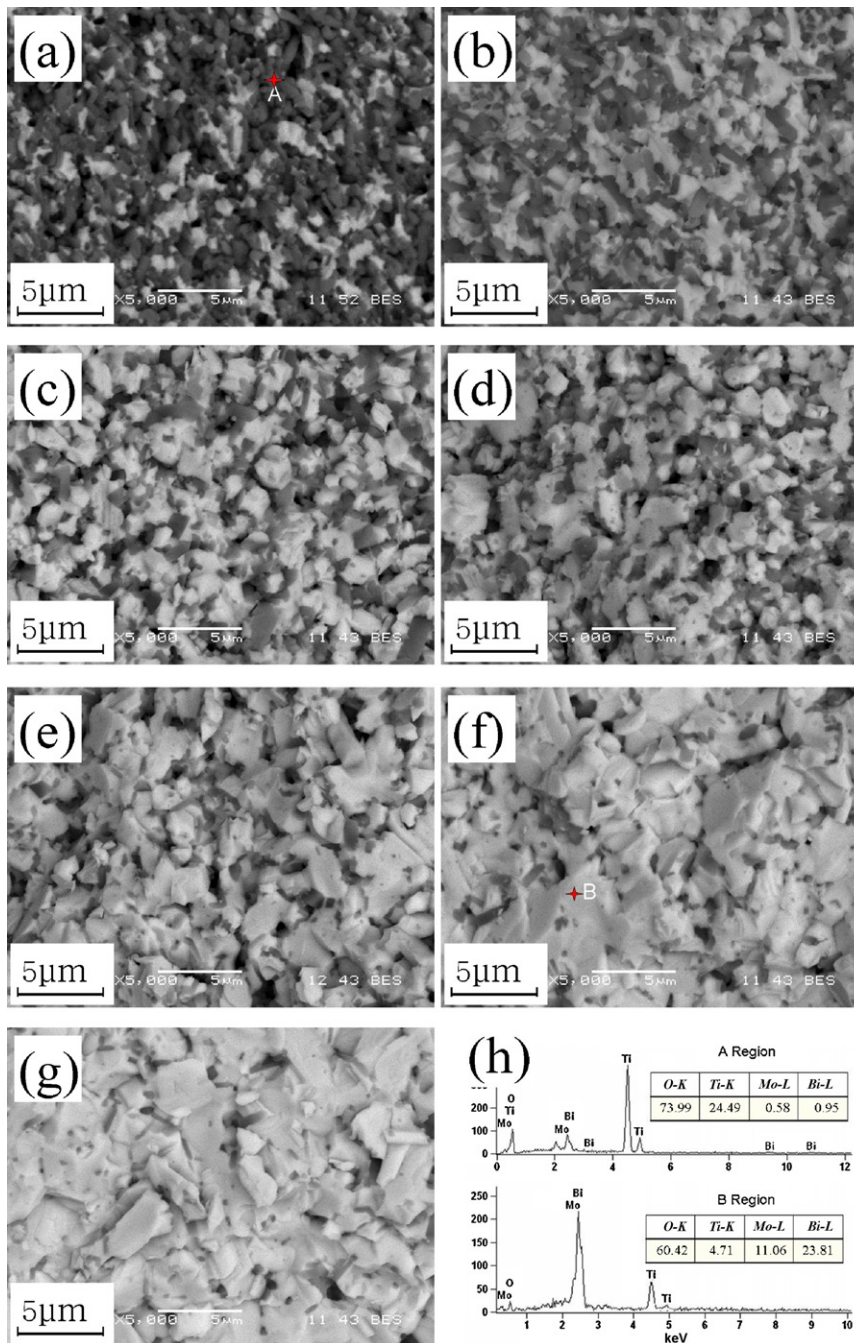


**Fig. 2.** Backscattered electron images and EDS analysis of the fracture surfaces of  $x\text{Bi}_2\text{MoO}_6-(1-x)\text{TiO}_2$  ceramics sintered at  $850^\circ\text{C}$  for 3 h: (a)  $x=0.06$ , (b)  $x=0.125$ , (c)  $x=0.21$ , (d)  $x=0.33$ , (e)  $x=0.50$ , (f)  $x=0.57$ , (g)  $x=0.65$ , (h) EDS pattern.

The mixing rule of  $\tau_f$  value could be obtained from the Lichtenecker empirical logarithmic rule of function (2). As being well known, the relationship between temperature coefficient of permittivity ( $\tau_\varepsilon$ ) and  $\tau_f$  is,

$$\tau_f = -\left(\frac{1}{2}\tau_\varepsilon + \alpha_L\right) \quad (3)$$

where  $\alpha_L$  is the linear thermal-expansion coefficient. The  $\tau_\varepsilon$  is defined as the following:

$$\tau_\varepsilon = \frac{1}{\varepsilon_r} \frac{d\varepsilon_r}{dT} = \frac{d(\lg\varepsilon_r)}{dT} = y_1 \frac{1}{\varepsilon_1} \frac{d\varepsilon_1}{dT} + y_2 \frac{1}{\varepsilon_2} \frac{d\varepsilon_2}{dT} = y_1 \tau_{\varepsilon 1} + y_2 \tau_{\varepsilon 2} \quad (4)$$

where  $\tau_{\varepsilon 1}$  and  $\tau_{\varepsilon 2}$  are the  $\tau_\varepsilon$  values of the  $\text{Bi}_2\text{MoO}_6$  phase and the rutile  $\text{TiO}_2$  phase, respectively. Thus, the mixing rule of  $\tau_f$  value

could be described like this:

$$\tau_f = y_1 \tau_{f1} + y_2 \tau_{f2} \quad (5)$$

where  $\tau_{f1}$  and  $\tau_{f2}$  are the  $\tau_f$  values of the  $\text{Bi}_2\text{MoO}_6$  phase and the rutile  $\text{TiO}_2$  phase, respectively. The theoretical  $\tau_f$  values of the  $x\text{Bi}_2\text{MoO}_6-(1-x)\text{TiO}_2$  composite ceramics were calculated using the function (5) and the results were listed in Table 1. Comparing the measured  $\tau_f$  with the theoretical value, it is seen that the measured  $\tau_f$  was a little more positive, which might result from the element diffusion in the  $x\text{Bi}_2\text{MoO}_6-(1-x)\text{TiO}_2$  compounds. The  $\tau_f$  value of the composite ceramic was tailored to near zero when  $x=0.57$ .

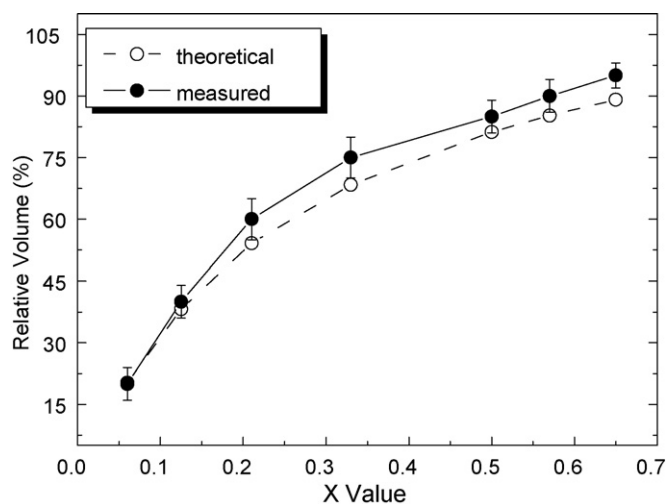


**Fig. 3.** Theoretical and measured volume fractions of  $\text{Bi}_2\text{MoO}_6$  phase in the ceramic matrix vs  $x$  value.

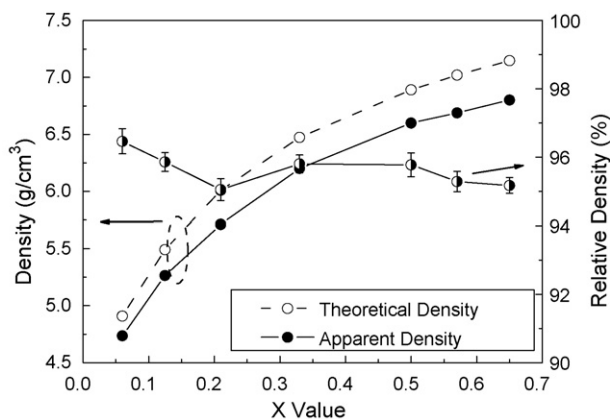


**Fig. 4.** Densities of  $x\text{Bi}_2\text{MoO}_6-(1-x)\text{TiO}_2$  composite ceramics sintered at  $850^\circ\text{C}$  for 3 h

#### 4. Conclusions

The  $x\text{Bi}_2\text{MoO}_6-(1-x)\text{TiO}_2$  composite ceramics were prepared by conventional solid state reaction method. All the ceramics could be well sintered at  $850^\circ\text{C}$  for 3 h. Tetragonal rutile phase and mon-

oclinic  $\text{Bi}_2\text{MoO}_6$  phase coexisted in the ceramics in the range from 0.06 to 0.65. In the  $\text{Bi}_2\text{MoO}_6$ -rich side of the compounds, Ti element diffused slightly into the  $\text{Bi}_2\text{MoO}_6$  grains and a solid solution with  $\text{Bi}_2\text{MoO}_6$  phase was formed in the compound. As the  $x$  value increased from 0.06 to 0.65, the permittivity changed from 77.5 to 33.5 and the  $\tau_f$  value shifted from  $+348.1$  to  $-37.8$  ppm/ $^\circ\text{C}$ . The temperature stable microwave dielectric ceramic was obtained when  $x=0.57$  in the  $x\text{Bi}_2\text{MoO}_6-(1-x)\text{TiO}_2$  system, and it showed excellent dielectric properties of  $\epsilon_r=36.7$ ,  $Q_f=16,800$  GHz and  $\tau_f=0$  ppm/ $^\circ\text{C}$ .

#### Acknowledgements

This work was supported by the National 973-project of China (2009CB623302) and National Project of International Science and Technology Collaboration (2009DFA51820).

#### References

- [1] R.R. Tummala, *J. Am. Ceram. Soc.* 74 (1991) 895–908.
- [2] M.T. Sebastian, H. Jantunen, *Int. Mater. Rev.* 53 (2008) 57–90.
- [3] K.W. Long, K.M. Luk, *IEEE Antenna Propag.* 43 (1995) 17–19.
- [4] C.L. Huang, R.J. Lin, J.H. Wang, *Jpn. J. Appl. Phys. Part1-Regular Papers Short Notes Rev. Papers* 41 (2002) 758–762.
- [5] D.W. Kim, B. Park, J.H. Chung, K.S. Hong, *Jpn. J. Appl. Phys.* 39 (2000) 2696–2700.
- [6] J.X. Tong, Q.L. Zhang, H. Yang, J.L. Zou, *Mater. Lett.* 59 (2005) 3252–3255.
- [7] T. Takada, S.F. Wang, S. Yoshikawa, S.T. Tang, R.E. Newnham, *J. Am. Ceram. Soc.* 77 (1994) 2485–2488.
- [8] J.R. Kim, D.W. Kim, H.S. Jung, K.S. Hong, *J. Eur. Ceram. Soc.* 26 (2006) 2105–2109.
- [9] S. George, M.T. Sebastian, *J. Alloys Compd.* 473 (2009) 336–340.
- [10] C.L. Huang, C.L. Pan, W.C. Lee, *J. Alloys Compd.* 462 (2008) 5–8.
- [11] J. Wang, Z.X. Yue, Z.L. Gui, L.T. Li, *J. Alloys Compd.* 392 (2005) 263–267.
- [12] V. Tolmer, G. Desgardin, *J. Am. Ceram. Soc.* 80 (1997) 1981–1991.
- [13] M.M.A. Sekar, K.C. Patil, *Mater. Sci. Eng. B* 38 (1996) 273–279.
- [14] M. Udovic, M. Valant, D. Suvorov, *J. Am. Ceram. Soc.* 87 (2004) 591–597.
- [15] M. Udovic, M. Valant, D. Suvorov, *J. Eur. Ceram. Soc.* 21 (2001) 1735–1738.
- [16] M. Valant, D. Suvorov, *J. Eur. Ceram. Soc.* 24 (2004) 1715–1719.
- [17] D.K. Kwon, M.T. Lanagan, T.R. Shrout, *Mater. Lett.* 61 (2007) 1827–1831.
- [18] D.K. Kwon, M.T. Lanagan, T.R. Shrout, *J. Ceram. Soc. Jpn.* 113 (2005) 216–219.
- [19] D.K. Kwon, M.T. Lanagan, T.R. Shrout, *J. Am. Ceram. Soc.* 88 (2005) 3419–3422.
- [20] A. Feteira, D.C. Sinclair, *J. Am. Ceram. Soc.* 91 (2008) 1338–1341.
- [21] G. Subodh, M.T. Sebastian, *J. Am. Ceram. Soc.* 90 (2007) 2266–2268.
- [22] D. Zhou, H. Wang, L.X. Pang, C.A. Randall, X. Yao, *J. Am. Ceram. Soc.* 92 (2009) 2242–2246.
- [23] K. Fukuda, R. Kitoh, I. Awai, *Jpn. J. Appl. Phys.* 32 (1993) 4584–4588.
- [24] C.F. Shih, W.M. Li, M.M. Lin, C.Y. Hsiao, K.T. Hung, *J. Alloys Compd.* 485 (2009) 408–412.
- [25] Y.C. Liou, Y.T. Chen, W.C. Tsai, *J. Alloys Compd.* 477 (2009) 537–542.
- [26] Y.G. Wu, X.H. Zhao, F. Li, Z.G. Fan, *J. Electroceram.* 11 (2003) 227–239.
- [27] S.J. Penn, N.M. Alford, A. Templeton, X. Wang, M. Xu, M. Reece, K. Schrapel, *J. Am. Ceram. Soc.* 80 (1997) 1885–1888.
- [28] H. Tamura, *Am. Ceram. Soc. Bull.* 73 (1994) 92–95.